JPE 9-2-16

ICPE'07 Selected Paper

Analytical Model of Conduction and Switching Losses of Matrix-*Z*-Source Converter

Keping You† and M. F. Rahman*

†*The School of Electrical Engineering and Telecommunications, The University of New South Wales, Australia

ABSTRACT

This paper investigates analytical models of Conduction and Switching Losses (CASLs) of a matrix-*Z*-source converter (MZC). Two analytical models of the CASLs are obtained through the examination of operating principles for a *Z*-source inverter and ac-dc matrix converter respectively. Based on the two models, the analytical model of CASLs for a MZC is constructed and visualized over a range of exemplified operating- points, each of which is defined by the combination of power factor (pf) and modulation index (*M*). The model provides a measurable way to approximate the total losses of the MZC.

Keywords: Conduction and Switching Losses, Matrix-Z-Source Converter, Analytical model of loss

1. Introduction

A matrix-*Z*-source converter (MZC) for bidirectional three-phase ac-dc power conversion was proposed marrying up both the advantages of the matrix converter and the *Z*-source inverter [1]. For a practical engineering development, MZC needs the investigation of conduction-and-switching-losses (CASLs) caused by its power-switch network. Nevertheless, the CASLs are essential measures in the comparison of merits between the MZC and existing bidirectional three-phase ac-dc power converters. The study of CASLs for MZC, therefore, is desirable and will be presented through analytical modeling in this paper.

The study of CASLs of a given power converter is usually carried out through a specific methodology using two elements, the operating principle of the converter and the CASLs model of each power-switch [2]-[9]. Section 2 briefly describes the operating principles of MZC, and Section 3 introduces the methodology of modeling CASLs and presents the parameters of CASLs for IGBT and Free-Wheeling Diode (FWD) as the base of modeling. Subsequently, sections 4 and 5 investigate the models of CASLs of *Z*-source inverter and ac-dc matrix converter respectively; section 6 then sets up the complete model of CASLs of MZC by using the two aforesaid models in sections 4 and 5.

2. Topology and Modulation Strategies of the Matrix-Z-source Converter

Detail Configuration of MZC may be found in [1] and is not reprinted here for brevity. MZC has two operating modes, the dc-ac inversion mode and the ac-dc rectification mode. Operating principles of each mode are briefly

Manuscript received January 30, 2009; revised Feb. 22, 2009
†Corresponding Author: youkeping@yahoo.com.au
Tel: +61- 2- 405136582, Fax:+61- 2- 93855993
*The School of Electrical Engineering and elecommunications, The University of New South Wales, Australia

described as follows.

2.1 Brief description of the operating principle of the MZC in dc-ac inversion mode

MZC has the same configuration as the Z-source inverter when MZC is in dc-ac inversion mode[1]. The Z-source inverter has the same structure of a power-switch network as that of VSI but with a different operating principle [10]. Fig. 1 shows the basic structure of a Z-source inverter. Its modeling and modulation strategy is given by (1)-(5) derived from Alesina-Venturini optimum PWM (AV-optimum PWM) [12] and [14]. In this modeling Maximum Constant Boost Control (MCBC) is employed[1]. Details of MCBC may be found in [11]. Fig. 4 in section 4 shows an example of the gate-drive logic and corresponding currents within one switching cycle.

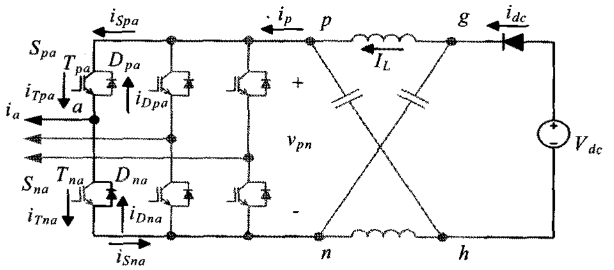

Fig. 1 Basic structure of Z-source inverter used in MZC when MZC is in dc-ac inversion mode

$$\begin{bmatrix} V_a(t) \\ V_b(t) \\ V_c(t) \end{bmatrix} = \begin{bmatrix} d_{pa} & d_{na} \\ d_{pb} & d_{nb} \\ d_{pc} & d_{nc} \end{bmatrix} B \begin{bmatrix} V_{dc}/2 \\ -V_{dc}/2 \end{bmatrix}$$
$$\frac{1}{B}\begin{bmatrix} I_p \\ -I_p \end{bmatrix} = \begin{bmatrix} d_{pa} & d_{pb} & d_{pc} \\ d_{na} & d_{nb} & d_{nc} \end{bmatrix} \begin{bmatrix} I_a(t) \\ I_b(t) \\ I_c(t) \end{bmatrix} \quad (1)$$

$$\begin{aligned} d_{pa} &= M[(1/2)\cos(\omega t) - (1/12)\cos(3\omega t)] + 1/2 \\ d_{pb} &= M[(1/2)\cos(\omega t - 2\pi/3) - (1/12)\cos(3\omega t)] + 1/2 \\ d_{pc} &= M[(1/2)\cos(\omega t + 2\pi/3) - (1/12)\cos(3\omega t)] + 1/2 \\ d_{na} &= 1 - d_{pa} \\ d_{nb} &= 1 - d_{pb} \\ d_{nc} &= 1 - d_{pc} \end{aligned} \quad (2)$$

$$B = 1/(\sqrt{3}M - 1) \quad 1/\sqrt{3} < M < 2/\sqrt{3} \quad (3)$$

$$D_0 = 1 - \frac{\sqrt{3}}{2}M \quad (4)$$

$$V_{pn} = BV_{dc} = \frac{1}{1-2D_0}V_{dc} = \frac{1}{\sqrt{3}M - 1}V_{dc} \quad (5)$$

where

$$\begin{bmatrix} V_a(t) \\ V_b(t) \\ V_c(t) \end{bmatrix} = \begin{bmatrix} V_{pk}\cos(\omega t) \\ V_{pk}\cos(\omega t - 2\pi/3) \\ V_{pk}\cos(\omega t + 2\pi/3) \end{bmatrix};$$

$$\begin{bmatrix} I_a(t) \\ I_b(t) \\ I_c(t) \end{bmatrix} = \begin{bmatrix} I_{pk}\cos(\omega t + \Phi) \\ I_{pk}\cos(\omega t - 2\pi/3 + \Phi) \\ I_{pk}\cos(\omega t + 2\pi/3 + \Phi) \end{bmatrix};$$

M is the modulation index; d_{ij} is the duty-cycle of switch S_{ij} (i=p,n, j=a,b,c); V_{pk} and I_{pk} are peak phase voltage and peak current respectively; I_p is the average dc-link current; V_{dc} is the dc source voltage; ω is the fundamental electric angular frequency; Φ is ac current phase angle; B is the boost factor; D_0 is shoot-through duty-cycle; V_{pn} is the peak dc-link voltage.

2.2 Brief description of the operating principle of the MZC in ac-dc rectification mode

MZC has the came configuration as ac-dc matrix when MZC is in the ac-dc rectification mode [1] as shown in Fig. 2. The operating principles using AV-optimum PWM may be described in (6)-(8) [1] and [13]. Fig. 5 and Fig. 6 in section 5 show an exemplified procedure of current commutation .

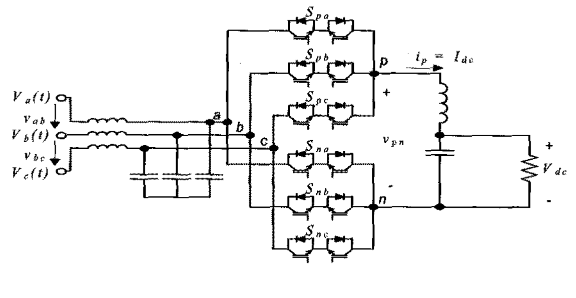

Fig. 2 Basic structure of ac-dc matrix converter used in MZC when MZC is in ac-dc rectification mode

$$\begin{bmatrix} V_{dc}/2 \\ -V_{dc}/2 \end{bmatrix} = \begin{bmatrix} d_{pa} & d_{pb} & d_{pc} \\ d_{na} & d_{nb} & d_{nc} \end{bmatrix} \begin{bmatrix} V_a(t) \\ V_b(t) \\ V_c(t) \end{bmatrix}; \quad \begin{bmatrix} I_a(t) \\ I_b(t) \\ I_c(t) \end{bmatrix} = \begin{bmatrix} d_{pa} & d_{na} \\ d_{pb} & d_{nb} \\ d_{pc} & d_{nc} \end{bmatrix} \begin{bmatrix} I_{dc} \\ -I_{dc} \end{bmatrix} \quad (6)$$

$$
\begin{aligned}
d_{pa} &= M\begin{bmatrix}(1/2)\cos(\omega_{in}t)+\\(7/36)\cos(2\omega_{in}t)-(1/36)\cos(4\omega_{in}t)\end{bmatrix}+1/3\\
d_{pb} &= M\begin{bmatrix}(1/2)\cos(\omega_{in}t-2\pi/3)+\\(7/36)\cos(2\omega_{in}t+2\pi/3)-(1/36)\cos(4\omega_{in}t)\end{bmatrix}+1/3\\
d_{pc} &= 1-d_{pa}(t)-d_{pb}(t)\\
d_{na} &= M\begin{bmatrix}(-1/2)\cos(\omega_{in}t)+\\(7/36)\cos(2\omega_{in}t)-(1/36)\cos(4\omega_{in}t)\end{bmatrix}+1/3\\
d_{nb} &= M\begin{bmatrix}(-1/2)\cos(\omega_{in}t-2\pi/3)+\\(7/36)\cos(2\omega_{in}t+2\pi/3)-(1/36)\cos(4\omega_{in}t)\end{bmatrix}+1/3\\
d_{nc} &= 1-d_{na}(t)-d_{nb}(t)
\end{aligned} \quad (7)
$$

$$
0 < M = \frac{4V_{dc}}{3\sqrt{3}V_{in}} < 2/\sqrt{3} \quad (8)
$$

Where,

$$
\begin{bmatrix}V_a(t)\\V_b(t)\\V_c(t)\end{bmatrix}=\begin{bmatrix}V_{in}\cos(\omega_{in}t)\\V_{in}\cos(\omega_{in}t-2\pi/3)\\V_{in}\cos(\omega_{in}t+2\pi/3)\end{bmatrix};
$$

$$
\begin{bmatrix}I_a(t)\\I_b(t)\\I_c(t)\end{bmatrix}=\begin{bmatrix}I_{in}\cos(\omega_{in}t+\Phi)\\I_{in}\cos(\omega_{in}t-2\pi/3+\Phi)\\I_{in}\cos(\omega_{in}t+2\pi/3+\Phi)\end{bmatrix};
$$

V_{in} and I_{in} are peak phase voltage and peak current respectively; ω_{in} is ac angular speed; Φ is input ac current phase angle; V_{dc} and I_{dc} are the output dc voltage and dc current respectively; d_{ij} ($i = p, n; j = a, b, c$) is duty-cycle.

3. Method of Modeling CASLs and Experimental Data to be Used

3.1 Methodology of modeling CASLs of power converters

The methodology may be grouped into two categories: one for dynamic electro thermal behavior and one for steady-state CASLs. The methodology for dynamic electrothermal behavior focuses on the power-switches in a given power converter; the relevant CASLs model of the power-switch is a physical-based model where the junction temperature is treated as a variable. Due to the complexity of the physical-based models, this methodology relies on simulation tools and has to focus on the study at a single operating-point [2],[3]. In the cases where the quick estimation of the CASLs of a power converter over a range of operating-points is required, this methodology may theoretically be used but will lead to an over complicated procedure. On the other hand, the methodology for steady-state CASLs focuses on the total CASLs of a power converter; the relevant CASLs model of the power-switch consists of an equivalent conduction-loss model and an equivalent switching-loss model. The junction temperature in this methodology is treated as a given unchangeable condition. Due to its simplicity, this methodology does not rely on simulation tools and is able to analytically express the approximated CASLs of a power converter over a range of operating-points [4], [9]. Within this methodology, on-state voltage/resistance and turn-on/off switching energy at a given junction temperature are critical to approximate the conduction loss and switching loss respectively. A powerful and fairly accurate way is to measure these parameters and then describe the dependency of the conduction loss or the switching loss on the applied voltage and/or current in a simple equation. The equation for the conduction loss is obvious. The equation for the switching loss, however, is obtained through various ways of approximation[4]-[6], [8]. A set of the measured on-state voltage/resistance and a quadratic least-square approximation of the dependency of the switching energy on the switched voltage/current were reported in [6] and verified through[7]. The experimental data will be employed in this paper where the quick estimation of CASLs of MZC over a range of operating-points is required.

3.2 Conduction-loss model approximation

Fig.3 shows the model of IGBT or FWD as the combined voltage source and resistor in series. The tested parameters reported in [6] are listed in Table 1.

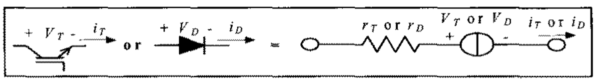

Fig. 3 Equivalent circuit of IGBT or FWD for calculating the conduction loss, where V_T is voltage drop of IGBT; V_D is forward voltage drop of FWD; r_T and r_D are on-state resistances of IGBT and free-wheel diode respectively

Table 1 Tested On-state parameters of IGBT and FWD at 120 °C of junction temperature

T_j	r_T	r_D	V_T	V_D
120°C	0.0787	0.038	0.768	0.732
Units	V/A	V/A	V	V

The switch devices under discussion are gated on/off by ideal PWM signals. The conduction-loss model within every switching cycle can be approximated as given by (9).

$$p_c = r_{T/D} i^2_{T/Drms} + v_{T/D} \langle i_{T/D} \rangle \quad (9)$$

where $i_{T/Drms}$ is the R.M.S. current within the switching cycle; $\langle i_{T/D} \rangle$ is the average current within the switching cycle.

3.3 Switching-loss model approximation

The Switching-loss model is obtained through averaging total energy losses caused by individual turn-on/off actions in a switching cycle. The dependency of the individual energy loss, w, on the switched voltage and switched current is given by (10) (11) (12). The turn-on energy loss of a diode is ignored.

$$w_{Toff}=K_{Toff1}ui+K_{Toff2}ui^2+K_{Toff3}u^2+K_{Toff4}u^2i+K_{Toff5}u^2i^2= w_{Toff}(u,i) \quad (10)$$

$$w_{Ton}=K_{Ton1}ui+ K_{Ton2}ui^2+ K_{Ton3}u^2+ K_{Ton4}u^2i+ K_{Ton5}u^2i^2 = w_{Ton}(u,i) \quad (11)$$

$$w_{Doff}=K_{Don1}ui+K_{Don2}ui^2+K_{Don3}u^2+K_{Don4}u^2i+K_{Don5}u^2i^2= w_{Doff}(u,i) \quad (12)$$

where u and i are the switched voltage and switched current respectively; T and D denote IGBT and FWD respectively; K_i (i = 1, 2, ...5) is the coefficient for approximation listed in Table 2 [6].

Table 2 Coefficients of the least-square approximation of the measured IGBT/FWD switching losses at 120 °C junction temperature (T_j) [6]

T_j		K_1	K_2	K_3	K_4	K_5
120° C	T_{off}	179	-1.31	0.650	-0.116	0.00348
	T_{on}	70.0	2.94	0.518	0.102	0.00155
	D_{off}	97.7	-3.73	0.488	0.140	0.00427
Units		nWs (VA)$^{-1}$	nWs (VA^2)$^{-1}$	nWs(V^2)$^{-1}$	nWs(V^{2}A)$^{-1}$	nWs(V^{2}A^2)$^{-1}$

4. Average CASLs Model of the Power-switch Network of Z-source Inverter

The analytical model of power loss for the Z-source inverter is developed in this section. The CASLs of the Z-source inverters is evenly distributed, hence, can be approximated by examining the CASLs of one pair of IGBT and its FWD, i.e. the T_{pa} and D_{na} shown in Fig. 1, where current i_a refers $I_a(t)$ of (1). Switching frequency is assumed much higher than the line frequency.

4.1 Conduction Loss model of Z-source Inverter

4.1.1 Conduction loss Caused by IGBT T_{pa} in Z-source Inverter

When the ac load current i_a is in the positive-half cycle, i.e. $i_a > 0$, within every switching cycle, the current crossing the T_{pa} consists of the shoot-through current and ac load current. Considering Fig. 4, one has (13) and (14) respectively.

$$\langle i_{Tpa} \rangle = D_0 \frac{2}{3} I_L + d_{pa} i_a \quad (13)$$

$$i^2_{Tparms} = D_0 (\frac{2}{3} I_L + \frac{i_a}{2})^2 + (d_{pa} - \frac{D_0}{2}) i_a^2 \quad (14)$$

where $\langle i_{Tpa} \rangle$ is the average current over switching cycle; i_{Tparms} is the R.M.S current over switching cycle; D_0 is the shoot-through duty-cycle; I_L is the average Z-source inductor current; d_{pa} is the duty-cycle of T_{pa}, i_a is the ac load current.

In the negative-half cycle, i.e. $i_a < 0$, only the shoot-through current crosses T_{pa} , as that of i_{Tna} in Fig. 4. The average and R.M.S. currents are

$$\langle i_{Tpa} \rangle = D_0 (\frac{2}{3} I_L + \frac{i_a}{2}) \quad (15)$$

$$i_{Tparms}^2 = D_0 (\frac{2}{3} I_L + \frac{i_a}{2})^2 \quad (16)$$

The average conduction loss caused by T_{pa} over line cycle, therefore, is given by (17)

$$P_{Tpa,c} = \frac{1}{2\pi}\int_{-\frac{\pi}{2}+\Phi}^{\frac{3\pi}{2}+\Phi} (r_T i^2_{Tparms} + V_T\langle i_{Tpa}\rangle) d\varphi$$

$$= r_T\left[\frac{1}{2\pi}\int_{-\frac{\pi}{2}+\Phi}^{\frac{3\pi}{2}+\Phi} D_0(\frac{2}{3}I_L + \frac{i_a}{2})^2 d\varphi + \frac{1}{2\pi}\int_{-\frac{\pi}{2}+\Phi}^{\frac{\pi}{2}+\Phi} (d_{pa} - \frac{D_0}{2}) i_a^2 d\varphi\right]$$

$$+ V_T\left[\frac{1}{2\pi}\int_{-\frac{\pi}{2}+\Phi}^{\frac{\pi}{2}+\Phi} (D_0\frac{2}{3}I_L + d_{pa} i_a) d\varphi + \frac{1}{2\pi}\int_{\frac{\pi}{2}+\Phi}^{\frac{3\pi}{2}+\Phi} D_0(\frac{2}{3}I_L + \frac{i_a}{2}) d\varphi\right] \quad (17)$$

where $\varphi = \omega t$; i_a is $I_a(t)$ in (1); D_0 was given by (4).

Replacing variables of i_a, d_{pa} and D_0 in (17). by those in (1), (2) and (4), after some trigonometric operation, the average conduction loss caused by IGBT T_{pa} may be approximated as given by (18), assuming that the power loss is significantly smaller than the active power flow in a proper designed Z-source converter.

$$P_{Tpa,c} = \left[\begin{array}{l} r_T\left(I_{pk}^2\left(\frac{1}{8} + \frac{M\cos\Phi}{3\pi} - \frac{M\cos 3\Phi}{90\pi}\right) + I_L^2\frac{2\left(2-\sqrt{3}M\right)}{9}\right) + \\ V_T\left(I_{pk}\left(\frac{1}{2\pi} + \frac{M\cos\Phi}{8}\right) + I_L\left(\frac{2-\sqrt{3}M}{2}\right)\right) \end{array}\right] \quad (18)$$

where,

$$I_L = \frac{P_o}{V_{dc}} \quad (19)$$

$$I_{pk} = \frac{4}{3}\frac{\sqrt{3}M - 1}{M\cos\Phi}\frac{P_o}{V_{dc}} \quad (20)$$

where I_L is the average Z-source inductor current; I_{pk} is peak ac load current; P_o is the active power; M, V_{dc} and Φ were defined in (1), (2) and (3).

4.1.2 Conduction loss caused by FWD D_{na} in Z-source Inverter

Only in the positive-half line cycle can the FWD D_{na} carry load current, as in Fig. 4. The average current and the R.M.S. current of i_{Dna} over switching cycle is given by (21) and (22).

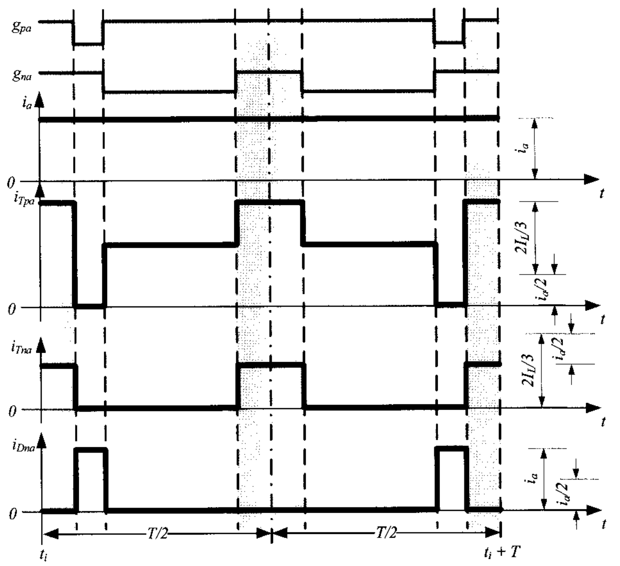

Fig. 4 Waveforms of T_{pa} and D_{na} of Fig.1 in one switching cycle when $i_a > 0$, where shadowed are shoot-through intervals. g_{pa} and g_{na} are gate-drive logic of T_{pa} and T_{na} respectively.

$$\langle i_{Dna}\rangle = (1 - d_{pa} - \frac{D_0}{2})i_a = (d_{na} - \frac{D_0}{2})i_a \quad (21)$$

$$i^2_{Dnarms} = (d_{na} - \frac{D_0}{2})i_a^2 \quad (22)$$

where $\langle i_{Dna}\rangle$ is the average current; i_{Dnarms} is the R.M.S current; d_{na} is the duty-cycle of D_{na}, i_a is the ac load current. Therefore, the average conduction loss caused by D_{na} over line cycle is given by (23).

$$P_{Dna,c} = \frac{1}{2\pi}\int_{-\frac{\pi}{2}+\Phi}^{\frac{\pi}{2}+\Phi} (r_D i^2_{Dnarms} + V_D\langle i_{Dna}\rangle) d\varphi$$

$$= r_D\left[\frac{1}{2\pi}\int_{-\frac{\pi}{2}+\Phi}^{\frac{\pi}{2}+\Phi} (d_{na} - \frac{D_0}{2}) i_a^2 d\varphi\right] + V_D\left[\frac{1}{2\pi}\int_{-\frac{\pi}{2}+\Phi}^{\frac{\pi}{2}+\Phi} (d_{na} - \frac{D_0}{2}) i_a d\varphi\right] \quad (23)$$

where $\varphi = \omega t$; Φ is ac current phase angle; $i_a = I_a(t)$. Replacing variables of d_{na}, i_a, in (23) by those in (1) and (2), after some trigonometric operation, the average conduction loss caused by free-wheel diode D_{na} can be approximated as given by (24).

$$P_{Dna,c}=\begin{bmatrix} r_D I_{pk}^{\;2}\left(\frac{1-D_0}{8}-\frac{M\cos\Phi}{3\pi}+\frac{M\cos 3\Phi}{90\pi}\right)+\\ V_D I_{pk}\left(\frac{1-D_0}{2\pi}-\frac{M\cos\Phi}{8}\right)\end{bmatrix} \tag{24}$$

where I_{pk} was given by (20).

4.1.3 Total average conduction loss in Z-source Inverter

Since the loss is evenly distributed in the power-switch network of the Z-source inverter, the total conduction loss can be approximated through (18) and (24) as given by (25).

$$\begin{aligned}P_{z,c}&=6\times(P_{Tpa,c}+P_{Dna,c})\\ &=6\times\begin{bmatrix} r_T I_{pk}^{\;2}\left(\frac{1}{8}+\frac{M\cos\Phi}{3\pi}-\frac{M\cos 3\Phi}{90\pi}\right)+r_T\left(\frac{2}{3}I_L\right)^2 D_0+\\ V_T I_{pk}\left(\frac{1}{2\pi}+\frac{M\cos\Phi}{8}\right)+V_T I_L D_0+\\ r_D I_{pk}^{\;2}\left(\frac{1-D_0}{8}-\frac{M\cos\Phi}{3\pi}+\frac{M\cos 3\Phi}{90\pi}\right)+\\ V_D I_{pk}\left(\frac{1-D_0}{2\pi}-\frac{M\cos\Phi}{8}\right)\end{bmatrix}\end{aligned} \tag{25}$$

where D_0, I_L and I_{pk} were given by (4), (19) and (20) respectively.

4.2 Switching loss model of Z-source Inverter

4.2.1 Switching loss caused by IGBT Tpa in Z-source Inverter

As shown in As shown in, when the ac load current is positive, i.e. $i_a > 0$, the T_{pa} in the Z-source inverter has four switching actions. Two of them, i.e. one turn-on and one turn-off in a non-shoot-through interval, are the same as that in an ordinary VSI, in which the switched voltage is the peak dc-link voltage and the switched current is the ac load current. The other two switching actions, one turn-on and one turn-off during the shoot-through interval, are imposed by the unique shoot-through actions. The switched voltage is still the peak dc-link voltage while the switched current is $2/3I_L+i_a/2$. Thus, the energy loss, w_1, within switching cycle can be approximated using (10) and (11), as given by (26).

$$w_1=w_{Tonoff}\left(V_{pn},\left(\frac{2}{3}I_L+\frac{i_a}{2}\right)\right)+w_{Tonoff}(V_{pn},i_a) \tag{26}$$

where w_1 is the energy loss of T_{pa} in a switching cycle when i_a is positive. w_{Tonoff} has the same form of $w_{off}(u,i)$ or $w_{on}(u,i)$ where the coefficients K_{Toni} or K_{Toffi} becomes $K_{Tonoffi}=K_{Toni}+K_{Toffi}$, $i = 1, 2, ..5$; V_{pn} is the peak dc-link voltage of Z-source inverter; I_L is in (19) ; i_a is the load current.

When ac load current is negative, i.e. $i_a < 0$, the T_{pa} carries the current in the same way as that of T_{na} with $i_a > 0$ in. Thus, switching actions of T_{pa} can be illustrated by i_{Tna} of T_{na} in Fig. 4. The waveform of i_{na} shows that the most left-hand turn-off is zero-voltage switching actions because the terminal voltage of T_{na} is clamped to almost zero voltage by the anti-parallel diode D_{na}, which matches the most right-hand turn-on. Hence, the relevant switching losses may be ignored. Only turn-on/off occurring in the middle position is taken into account. From the approximation model in (10) and (11), one has

$$w_2=w_{Tonoff}\left(V_{pn},\left(\frac{2}{3}I_L+\frac{i_a}{2}\right)\right) \tag{27}$$

where w_2 is the switching energy loss of T_{pa} per PWM cycle in the negative-half cycle; w_{Tonoff} was defined in (26). Thus

$$\begin{aligned}P_{Tpa,sw}&=f_{sw}\left[\frac{1}{2\pi}\int_{-\frac{\pi}{2}+\Phi}^{\frac{3\pi}{2}+\Phi}(w_1+w_2)d\varphi\right]\\ &=f_{sw}\begin{bmatrix}\frac{1}{2\pi}\int_{-\frac{\pi}{2}+\Phi}^{\frac{3\pi}{2}+\Phi} w_{Tonoff}\left(V_{pn},\left(\frac{2}{3}I_L+\frac{i_a}{2}\right)\right)d\varphi\\ +\frac{1}{2\pi}\int_{-\frac{\pi}{2}+\Phi}^{\frac{\pi}{2}+\Phi} w_{Tonoff}(V_{pn},i_a)d\varphi\end{bmatrix}\end{aligned} \tag{28}$$

where $P_{Tpa,sw}$ is the average switching loss in one line cycle. Replacing i_a by that in (1) and (2) with some trigonometric operation,

$$P_{Tpa,sw} = f_{sw}\begin{bmatrix} \frac{3}{2}K_{T3}V_{pn}^2 + (K_{T1}V_{pn} + K_{T4}V_{pn}^2)(\frac{3}{2\pi}I_{pk} + \frac{2}{3}I_L) \\ +(K_{T2}V_{pn} + K_{T5}V_{pn}^2)(\frac{1}{\pi}I_{pk}I_L + \frac{5}{16}I_{pk}^2 + \frac{4}{9}I_L^2) \end{bmatrix} \quad (29)$$

where $K_{Ti}=K_{Ton,i}+K_{Toff,i}$, i=1,2,..5; f_{sw} is the switching frequency; V_{pn}, I_L and I_{pk} were given by (5), (19) and (20) respectively.

4.2.2 Switching loss cause by Diode Dna in Z-source Inverter

D_{na} carries current only in the positive half cycle of load current. The turn-on switching loss of a diode is ignored. The waveform of i_{Dna} in Fig. 4 shows that the most right-hand turn-off of the diode is a zero-voltage turn-off due to the switched voltage clamped by T_{na}, hence, the relevant switching loss is ignored. Thus, only the turn-off at the left-hand contributes to switching loss energy

$$w_{Doff} = w_{Doff}(V_{pn}, i_a) \quad (30)$$

where V_{pn} was given in (5); i_a is the load current.

The average switching power loss of D_{na} in one line-cycle is

$$P_{Dna,sw} = f_{sw}\left[\frac{1}{2\pi}\int_{-\frac{\pi}{2}+\Phi}^{\frac{3\pi}{2}+\Phi} w_{Doff}\,d\varphi\right] = f_{sw}\left[\frac{1}{2\pi}\int_{-\frac{\pi}{2}+\Phi}^{\frac{\pi}{2}+\Phi} w_{Doff}\,d\varphi\right] = f_{sw}\left[\frac{1}{2\pi}\int_{-\frac{\pi}{2}+\Phi}^{\frac{\pi}{2}+\Phi} w_{Doff}(V_{pn}, i_a)\,d\varphi\right] \quad (31)$$

Replacing i_a by the $I_a(t)$ in (1), the average switching power loss of the FWD can be approximated by (32).

$$P_{Dna,sw} = f_{sw}\begin{bmatrix} K_{D3}V_{pn}^2 + (K_{D1}V_{pn} + K_{D4}V_{pn}^2)\frac{1}{\pi}I_{pk} \\ +(K_{D2}V_{pn} + K_{D5}V_{pn}^2)\frac{1}{4}I_{pk}^2 \end{bmatrix} \quad (32)$$

where $K_{Di}=K_{Doff,i}$, $i=1,2,..5$; f_{sw} is the switching frequency; V_{pn} and I_{pk} were given by (5) and (20) respectively.

4.2.3 Total average switching loss in Z-source Inverter

Since the switching power loss is evenly distributed, the total average switching loss can be approximated by

$$P_{z,sw} = 6\times(P_{Tpa,sw} + P_{Dna,sw}) = 6\times f_{sw}\begin{bmatrix} \frac{3}{2}K_{T3}V_{pn}^2 + \left(K_{T1}V_{pn} + K_{T4}V_{pn}^2\right)\left(\frac{3}{2\pi}I_{pk} + \frac{2}{3}I_L\right) + \\ (K_{T2}V_{pn} + K_{T5}V_{pn}^2)\left(\frac{1}{\pi}I_{pk}I_L + \frac{5}{16}I_{pk}^2 + \frac{4}{9}I_L^2\right) + \\ K_{D3}V_{pn}^2 + \left(K_{D1}V_{pn} + K_{D4}V_{pn}^2\right)\frac{1}{\pi}I_{pk} + \\ (K_{D2}V_{pn} + K_{D5}V_{pn}^2)\frac{1}{4}I_{pk}^2 \end{bmatrix} \quad (33)$$

where parameters have been defined in (29) And (32).

5. Average CASLs Model of the Three-phase ac-dc Matrix Converter

5.1 Average conduction-loss model of ac-dc matrix converter

It is well known that ac load current dominates the average conduction loss of an ac-ac matrix converter. For the case of ac-dc matrix, dc load current dominates

$$P_{mc,c} = 2[(V_T + V_D)I_{dc} + (r_T + r_D)I_{dc}^2] \quad (34)$$

where $P_{mc,c}$ is the average conduction loss; the square bracketed item is the conduction loss per output phase.

5.2 Average switching loss model of ac-dc matrix converter

The model of switching loss of ac-dc matrix converter is not as obvious as that of the conduction loss. For the convenience of discussion, Fig. 5 presents the timing diagram of a switching cycle in an arbitrary 60°-sector of line-cycle; Fig. 6 illustrates the detail switching actions within the commutation period T_{CM} immediately after the instant t_{CMp1} in Fig. 5. The basic condition for the discussion is that the sequence of current commutation is in the way of "$a\rightarrow b\rightarrow cc\rightarrow b\rightarrow a$" all the time as shown in Fig. 5, and that the four-step method in Fig. 6 is used for every commutation. The ac source is assumed three-phase balanced. Gate-drives for individual switches are assumed ideal and lossless. Switched voltage that is equal to the forward voltage drop of IGBT or FWD does not contribute to switching loss.

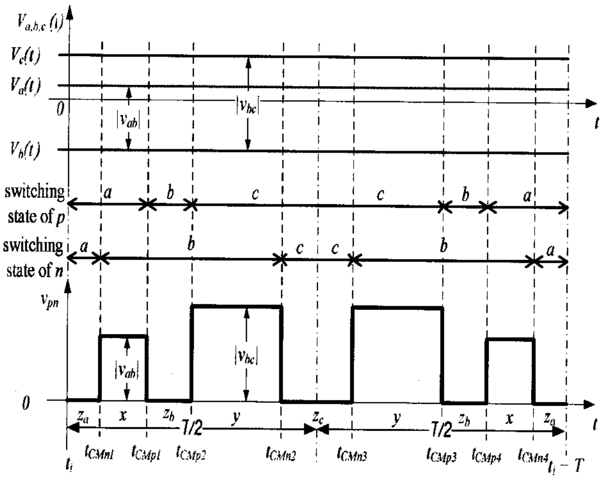

Fig. 5 One instance of switching states of the circuit in Fig.2 in one switching cycle T, where x and y are the intervals of active states; z_a, z_b, and z_c are the ones of zero-states; t_{CMpi} and t_{CMni} (i = 1, 2, 3, 4) are the instants of current commutation of phase p and n respectively

At instant t_{CMp1} in the left-hand half switching cycle of Fig. 5, when i_p commutates from phase a to b, the switching actions are the turn-off of the switch-cell S_{pa} and the turn-on of S_{pb}; no switching action occurs in the switch-cell S_{pc}; the switched voltage is v_{ab}. Examining Fig. 6. shows that, when i_p is positive, i.e. the forward current, the turn-off of the backward switch S_{paB} at t_1 is a zero-current turn-off (ZC-off) not producing switching loss due to the absence of backward current; the turn-on of the forward switch S_{pbF} at t_2 is a zero-current turn-on (ZC-on) not producing switching loss because its reversed terminal voltage under the condition of line voltages ($V_a(t)>V_b(t)$) blocks the forward current during the turn-on; the turn-off of the forward switch S_{paF} at t_3 is a non-zero-current turn-off (NZC-off) certainly producing switching loss due to the existence of switched current; the turn-on of the backward switch S_{pbB} at t_4 is a ZC-on not producing switching loss due to the absence of backward current. At instant t_{CMp4} with the same switched voltage of v_{ab}, by symmetry of the switching states as shown in Fig. 5, switch-cell S_{pa} produces the switching loss through a non-zero-current turn-on (NZC-on) of forward switch S_{paF} when the forward current i_p commutates from phase b back to a. Similar examination applied to the two instants at t_{CMp2} and t_{CMp3} shows that the NZC-on and NZC-off occur in the switch-cell S_{pc}, and produce switching loss at the two instants respectively when forward current commutates between phase b and c with the switched voltage of v_{bc}. Details of the examination are ignored for abbreviation. Thus, with the common switched current, two combinations of NZC-on and NZC-off produce switching loss with two switched voltages v_{ab} and v_{bc} respectively.

Note that the switching cycle and 60°-sector of line-cycle are arbitrarily selected in the aforementioned examination, and that the line-to-line voltage v_{ca} has no chance to be the switched voltage due to the definite absence of the current commutation between phase a and c for the given commutation sequence of "$a \rightarrow b \rightarrow cc \rightarrow b \rightarrow a$" all the time. The examination may be applied to the other 60°-sectors, revealing that the difference in the switching actions between different sectors is merely the way how the two combinations of the NZC-on and NZC-off are allocated, as shown in Table 3. Considering the IGBTs and FWDs used in the switch-cells are identical, the common facts from the examination about the switching loss of output phase p with forward current is that the switching loss is caused by two and only two combinations of NZC-on and NZC-off at switched voltages v_{ab} and v_{bc} respectively.

Therefore, using (10), (11), and (12), switching energy within one switching cycle in the output phase p may be approximated as given by (35).

$$\begin{aligned} w_{sw} &= \begin{bmatrix} w_{Ton}(v_{ab},I_{dc})+w_{Toff}(v_{ab},I_{dc})+w_{Doff}(v_{ab},I_{dc})+ \\ w_{Ton}(v_{bc},I_{dc})+w_{Toff}(v_{bc},I_{dc})+w_{Doff}(v_{bc},I_{dc}) \end{bmatrix} \\ &= w_{TonoffDoff}(v_{ab},I_{dc})+w_{TonoffDoff}(v_{bc},I_{dc}) \\ &= w_{sw}(K_i,v_{ab},I_{dc})+w_{sw}(K_i,v_{bc},I_{dc}) \end{aligned} \tag{35}$$

where $K_i = K_{iTon} + K_{iToff} + K_{iDoff}$; K_{iTon}, K_{iToff}, and K_{iDoff} are in Table 2(i = 1, 2, ..5); $w_{sw}(K_i, v_{ab}, I_{dc})$ and $w_{sw}(K_i, v_{bc}, I_{dc})$ are the switching energy loss when switched voltage are v_{ab}, and v_{bc} respectively; I_{dc} is the forward current equal to the output dc current. From the model (6), v_{ab} and v_{bc} are

$$v_{ab} = \sqrt{3}V_{in}\cos(\varphi_{in} + \pi/6); \quad v_{bc} = \sqrt{3}V_{in}\cos(\varphi_{in} - \pi/2) \tag{36}$$

where $\varphi_{in} = \omega_{in}t$; ω_{in} and V_{in} were defined in (6).

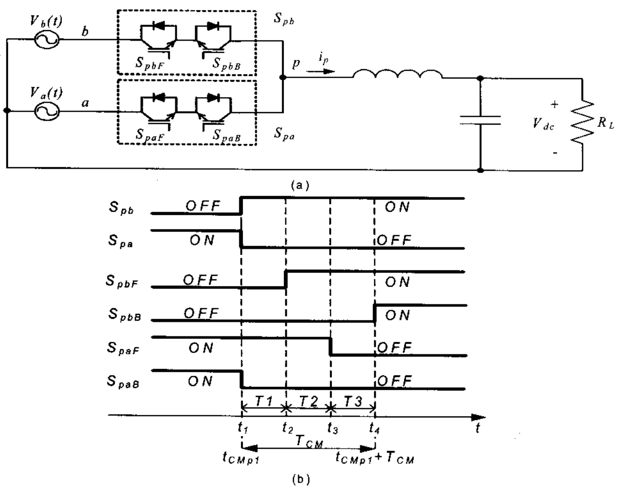

Fig. 6 Illustration of four-step commutation at the instant t_{CMp1} in Fig. 5 when the forward current of output phase p commutates from phase a to b (a) the simplified circuit, where each physical switch is comprised of a combination of one IGBT and one FWD in series; F and B denote forward and backward respectively. (b) the timing diagram of four-step commutation, where S_{pa} and S_{pb} are logic signals for switch-cells; S_{pjk} ($j = a, b$; $k = F, B$) are on/off states of the physical switches; T_{CM} is the commutation period.

Table 3 Feature of switching actions of the switch-cells connected to the output phase p in each 60°-sector of line-cycle according to the given sequence of current commutation and the four-step commutation method

	Sectors	Switch-cells	a→b	b→c	c→b	b→a
1	$v_a > v_b > v_c$	S_{pa}	NZC-off			NZC-on
		S_{pb}	ZC-on	NZC-off	NZC-on	ZC-off
		S_{pc}		ZC-on	ZC-off	
2	$v_b > v_c > v_a$	S_{pa}	ZC -off			ZC -on
		S_{pb}	NZC -on	NZC-off	NZC-on	NZC -off
		S_{pc}		ZC-on	ZC-off	
3	$v_c > v_a > v_b$	S_{pa}	NZC -off			NZC -on
		S_{pb}	ZC -on	ZC-off	ZC-on	ZC -off
		S_{pc}		NZC-on	NZC-off	
4	$v_c > v_b > v_a$	S_{pa}	ZC -off			ZC -on
		S_{pb}	NZC -on	ZC-off	ZC-on	NZC -off
		S_{pc}		NZC-on	NZC-off	
5	$v_b > v_a > v_c$	S_{pa}	ZC -off			ZC -on
		S_{pb}	NZC -on	NZC-off	NZC-on	NZC -off
		S_{pc}		ZC-on	ZC-off	
6	$v_a > v_c > v_b$	S_{pa}	NZC -off			NZC -on
		S_{pb}	ZC -on	ZC-off	ZC-on	ZC -off
		S_{pc}		NZC-on	NZC-off	

From (35) and(36), by some trigonometric operation, the average switching loss in the output phase p in one switching cycle, p_{swsw}, can be approximated as given by (37).

$$\begin{aligned} p_{swsw} &= f_{sw} w_{sw} \\ &= f_{sw}\left(w_{sw}(K_i, v_{ab}, I_{dc}) + w_{sw}(K_i, v_{bc}, I_{dc})\right) \\ &= A\sqrt{3}V_{in}\cos(\varphi_{in} - \pi/6) + 3BV_{in}^2(1 - 0.5\cos 2(\varphi_{in} - \pi/6)) \end{aligned} \tag{37}$$

where f_{sw} is the switching frequency; $A = K_1 I_{dc} + K_2 I_{dc}^2$ and $B = K_3 + K_4 I_{dc} + K_5 I_{dc}^2$; K_i ($i = 1, 2, ...5$) were defined in (35); $\varphi_{in} = \omega_{in}t$; ω_{in} and V_{in} were defined in (6).

The average switching loss in the output phase p in one line-cycle, p_{swph}, is

$$p_{swph} = \frac{1}{2\pi}\int_0^{2\pi} p_{swsw} d\varphi_{in} = \frac{3}{\pi}\int_{-\pi/6}^{\pi/6} p_{swsw} d\varphi_{in} = f_{sw}(1.43AV_{in} + 2.38BV_{in}^2) \tag{38}$$

where A and B were defined in (37); V_{in} was defined in (6).

The average switching loss in output phase n is the same as that in output phase p because of the balanced input voltages and the identical switch-cells. Therefore, the average switching power loss of the whole ac-dc matrix converter is

$$P_{mc,sw} = 2\times p_{swph} = f_{sw}\begin{bmatrix} 4.76K_3V_{in}^2 + (2.86K_1V_{in} + 4.76K_4V_{in}^2)I_{dc} \\ +(2.86K_2V_{in} + 4.76K_5V_{in}^2)I_{dc}^2 \end{bmatrix} \quad (39)$$

where K_i ($i = 1, 2, ...5$) were defined in (35); f_{sw} is the switching frequency; I_{dc} and V_{in} were defined in (6). Thus, the average switching power loss, $P_{mc,sw}$, of the whole ac-dc matrix converter has dependency on output dc load current and input ac peak phase voltage. Considering the relation in (8), one has

$$V_{in} = 4V_{dc}/(3\sqrt{3}M) \quad (40)$$

Replacing V_{in} in (39) with that in (40), the $P_{mc,sw}$ becomes

$$P_{mc,sw} = f_{sw}\begin{bmatrix} \frac{2.12K_3V_{dc}^2}{3/4M^2} + I_{dc}(\frac{1.91K_1V_{dc}}{\sqrt{3}/2M} + \frac{2.12K_4V_{dc}^2}{3/4M^2}) \\ +I_{dc}^2(\frac{1.91K_2V_{dc}}{\sqrt{3}/2M} + \frac{2.12K_5V_{dc}^2}{3/4M^2}) \end{bmatrix} \quad (41)$$

where f_{sw} is the switching frequency; I_{dc} and V_{dc} were defined in (6), and M in (8).

It can be seen from (34) and (41) that the conduction and switching losses in an ac-dc matrix converter has no dependency on cos(Φ), i.e. the power factor (pf).

6. Average CASLs Model of the Proposed MZC

Thus far, the power loss approximation has been investigated for power-switch network in a *Z*-source inverter or ac-dc matrix converter. MZC marries up both structures of *Z*-source inverter and ac-dc matrix converter. Therefore, its power loss approximation for the power-switch network can be examined now. Table 4 shows the conditions for the calculation. The calculated results will be converted into the form of "mWatts per Watt" as given by (42) for the convenience of visualization.

$$P'_{loss} = \frac{P_{loss}}{P_o}\times 1000 \quad (42)$$

where P'_{loss} is the result to be visualized; P_{loss} is the calculated loss at certain operating point indicated by a pair of modulation index (M) and power factor (pf) in Table; P_o is defined in Table 4.

Table 4 Conditions for the calculation of power loss using the analytical model of conduction and switching losses of MZC

Symbol	Description	Values	
		For dc-ac inversion	For ac-dc rectification
pf	cos(Φ)	0.7 < pf < 1.0	0.7 < pf < 0.9
M	Modulation index	0.866 < *M* < 1.155	0.5 < *M* < 1.155
V_{dc}	dc voltage	36 V	42 V
P_o	Active power	2000 W	2000 W
f_{sw}	Switching frequency	10 kHz	10 Hz

6.1 Average CASLs Model of the proposed MZC in dc-ac inversion mode

6.1.1 Average conduction loss of the proposed MZC in dc-ac inversion mode

In dc-ac operation mode, the MZC operates as a *Z*-source inverter in which each switch consists of two common-emitter connected IGBTs with respective anti-paralleled FWDs. One of the two IGBTs is set at on-state all the time, and the other one serves as an active IGBT as shown in Fig. 7(a) [1]. Fig. 7(b) presents the equivalent configuration. Fig. 7 (c) shows the equivalent model during the on-state of the active IGBT. For this reason, the V_T, V_D, r_T, and r_D, used in (18)–(25) for the approximation of average conduction loss are replaced by V_{T+D}, V_{D+T}, r_{T+D}, and r_{D+T} respectively. V_{T+D}, V_{D+T}, r_{T+D}, and r_{D+T} are given by (43) and (44).

$$V_{T+D} = V_{D+T} = V_T + V_D \quad (43)$$

$$r_{T+D} = r_{D+T} = r_T + r_D \quad (44)$$

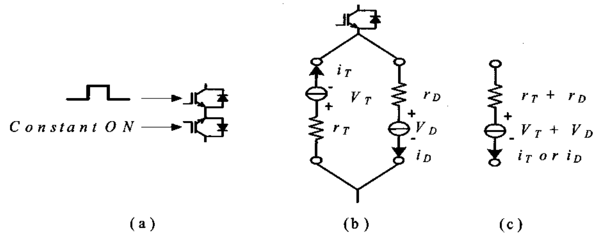

Fig. 7 Equivalent model of IGBT and FWD in MZC when MZC is in dc-ac inversion mode, (a) illustrative gate-drive signals and common-emitter IGBT-pair, (b) active switching IGBT and the model of constant-on IGBT, (c) model of whole common-emitter IGBT-pair

Equations (18) and (24) share the same parameters, hence the average conduction loss of Z-source inverter given by (25) can be arranged in (45)

$$P_{mzc-dcac,c} = 6\times\begin{bmatrix} r_{T+D} I_{pk}^2\left(\frac{2-D_0}{8}\right) + r_{T+D}\left(\frac{2}{3}I_L\right)^2 D_0 + \\ V_{T+D} I_{pk}\left(\frac{2-D_0}{2\pi}\right) + V_{T+D} I_L D_0 \end{bmatrix} \tag{45}$$

Where

$$I_L = \frac{P_o}{V_{dc}};\; I_{pk} = \frac{4(\sqrt{3}M-1)P_o}{3MV_{dc}\cos\Phi};\; D_0 = 1-\frac{\sqrt{3}M}{2}$$

The calculated result using the given values for dc-ac inversion in Table 4 is visualized in Fig. 8(a1).

6.1.2 Average switching loss of the proposed MZC in dc-ac inversion mode

MZC in dc-ac inversion mode operates as the Z-source inverter. The average switching loss then can be approximated by (29), (32), and (33). One has Switching loss caused by IGBT T_{pa}

$$P_{mzc-dcacTpa,sw} = f_{sw}\begin{bmatrix} \frac{3}{2}K_{T3}V_{pn}^2 + (K_{T1}V_{pn} + K_{T4}V_{pn}^2)(\frac{3}{2\pi}I_{pk} + \frac{2}{3}I_L) \\ +(K_{T2}V_{pn} + K_{T5}V_{pn}^2)(\frac{1}{\pi}I_{pk}I_L + \frac{5}{16}I_{pk}^2 + \frac{4}{9}I_L^2) \end{bmatrix} \tag{46}$$

where K_{Ti} $(i=1,2,..)$ is no longer the same one in (29) the one in the following expression because of the extra diode in series with T_{pa}, shown in Fig.7.

$$K_{Ti} = K_{Ton,i} + K_{Toff,i} + K_{Doff,i} \tag{47}$$

Switching loss caused by FWD D_{na} is

$$P_{mzc-dcacDna,sw} = f_{sw}\begin{bmatrix} K_{D3}V_{pn}^2 + (K_{D1}V_{pn} + K_{D4}V_{pn}^2)\frac{1}{\pi}I_{pk} \\ +(K_{D2}V_{pn} + K_{D5}V_{pn}^2)\frac{1}{4}I_{pk}^2 \end{bmatrix} \tag{48}$$

where $K_{Di}=K_{Doff,i}$ $(i=1,2,..)$ is the same as defined (32), since the constant on-state IGBT in series with the diode is merely offering a conduction path without active switching actions. The model for the approximation of the average switching loss of MZC in dc-ac inversion is

$$P_{mzc-dcac,sw} = 6\times(P_{mzc-dcacTpa,sw} + P_{mzc-dcacDna,sw})$$
$$= 6\times f_{sw}\left\{\begin{bmatrix} \frac{3}{2}K_{T3}V_{pn}^2 + (K_{T1}V_{pn} + K_{T4}V_{pn}^2)(\frac{3}{2\pi}I_{pk} + \frac{2}{3}I_L) \\ +(K_{T2}V_{pn} + K_{T5}V_{pn}^2)(\frac{1}{\pi}I_{pk}I_L + \frac{5}{16}I_{pk}^2 + \frac{4}{9}I_L^2) \end{bmatrix} + \begin{bmatrix} K_{D3}V_{pn}^2 + (K_{D1}V_{pn} + K_{D4}V_{pn}^2)\frac{1}{\pi}I_{pk} \\ +(K_{D2}V_{pn} + K_{D5}V_{pn}^2)\frac{1}{4}I_{pk}^2 \end{bmatrix}\right\} \tag{49}$$

where

$$I_L = \frac{P_o}{V_{dc}};\; I_{pk} = \frac{4}{3}\frac{\sqrt{3}M-1}{M\cos\Phi}P_o;\; V_{pn} = \frac{1}{\sqrt{3}M-1}V_{dc}$$

The calculated result using the given values for dc-ac inversion in Table 4 is visualized in Fig. 8(a2).

6.1.3 Average CASLs of MZC in dc-ac mode

By the results in the previous two sub-sections, the total average loss caused by power semiconductors in dc-ac mode of MZC can be approximated as given by (50).

$$P_{mzc-dcac} = P_{mzc-dcac,c} + P_{mzc-dcac,sw} \tag{50}$$

where $P_{mzc-dcac,c}$ and $P_{mzc-dcac,sw}$ are given in (45) and (49) respectively. The calculated result using the given values for dc-ac inversion in Table 4 is visualized in Fig. 8(a3).

6.2 Average CASLs Model of the proposed MZC in ac-dc rectification mode

In ac-dc rectification, the MZC is operated as ac-dc matrix converter shown in Fig. 2. The conduction loss and switching loss models of ac-dc matrix converter in (34) and (41) of section 5 can be used straightaway. The conduction loss $P_{mzc-acdc,c}$, switching loss $P_{mzc-acdc,sw}$, and CASLs $P_{mzc-acdc}$ of MZC in ac-dc rectification mode are given by(51), (52), and (53) respectively.

$$P_{mzc-acdc,c} = P_{mc,c} = 2[(V_T + V_D)I_{dc} + (r_T + r_D)I_{dc}^2] \tag{51}$$

$$P_{mzc-acdc,sw} = P_{mc,sw} = f_{sw}\left[\begin{array}{c} \frac{2.12K_3V_{dc}^2}{3/4M^2} + I_{dc}\left(\frac{1.91K_1V_{dc}}{\sqrt{3}/2M} + \frac{2.12K_4V_{dc}^2}{3/4M^2}\right) \\ + I_{dc}^2\left(\frac{1.91K_2V_{dc}}{\sqrt{3}/2M} + \frac{2.12K_5V_{dc}^2}{3/4M^2}\right) \end{array}\right] \tag{52}$$

$$P_{mzc-acdc} = P_{mzc-acdc,c} + P_{mzc-acdc,sw} \tag{53}$$

where V_{dc} and I_{dc} are dc voltage and dc current respectively; M is modulation index, $0 < M < 2/\sqrt{3}$; $K_i = K_{Ton,i} + K_{Toff,i} + K_{Doff,i}$ is the switching loss parameters given by Table 2; r_T, r_D, v_T, and v_D are On-state parameters given by Table 1.

Fig. 8(b1 - b3) are the visualized results of conduction loss, switching loss, and CASLs of MZC in the condition of ac-dc rectification mode in Table 4, in which dc voltage is 42 V.

7. Conclusion

The analytical models for the approximation of the conduction and switching losses of the power-switch network in the MZC have been achieved.

When the MZC is in dc-ac inversion mode, the analytical model for MZC is the same as that for the Z-source inverter except that the parameters of on-state resistance and forward voltage drop used in the approximation of conduction loss for MZC are higher than those for the Z-source inverter.

When the MZC is in ac-dc rectification mode, both the analytical models and the parameters in calculation are the same as that for the ac-dc matrix converter.

For the practice of engineering design work, the models developed in this paper are ready for use in the estimation of CASLs of Z-source inverters, ac-dc matrix converters, or MZC, after the acquisition of the experimental data of the on-state and switching energy of employed power-switches.

References

[1] Keping You, M. F. Rahman, "A matrix-Z-source converter for automotive integrated starter alternator system", Applied Power Electronics Conference and Exposition, 2008. APEC 2008. Twenty-Third Annual IEEE, pp. 273 – 279, 24-28 Feb. 2008.

[2] Mantooth H.A., Hefner A.R. Jr., "Electrothermal simulation of an IGBT PWM inverter", *Power Electronics, IEEE Transactions on*, Vol. 12, Issue 3, pp. 474-484, May 1997.

[3] Zhou, Z, Khanniche, M.S, Igic, P, Kong, S.T, Towers, M, Mawby, P., "A fast power loss calculation method

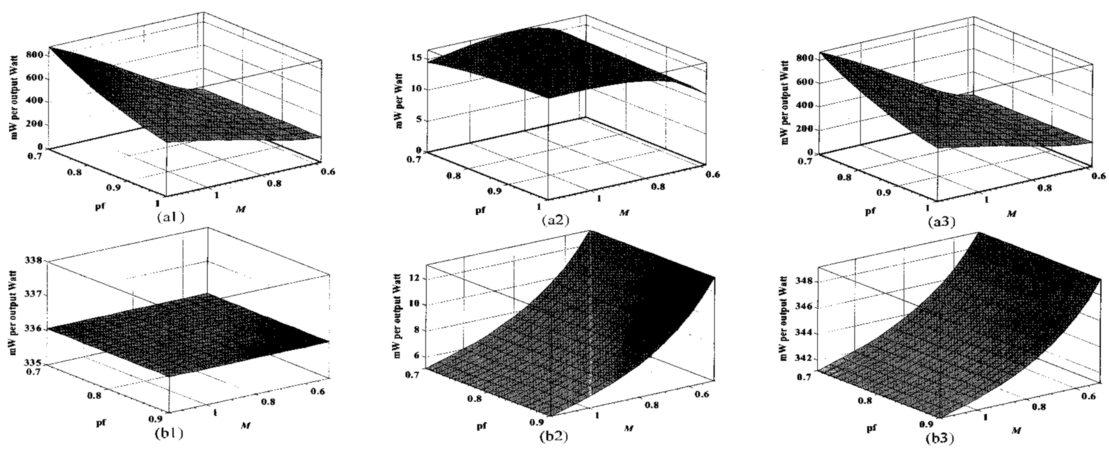

Fig. 8 Visualized losses of MZC. (a1), (a2), and (a3) are conduction loss, switching loss, and CASLs of MZC respectively when V_{dc} = 36 V in dc-ac inversion mode; (b1), (b2), and (b3) are conduction loss, switching loss, and CASLs of MZC respectively when V_{dc} = 42 V in ac-dc rectification mode.

for long real time thermal simulation of IGBT modules for a three-phase inverter system", Power Electronics and Applications, 2005 European Conference, pp. 9, 11-14 Sept. 2005.

[4] Bernet, S, Ponnaluri, S, Teichmann, R, "Design and loss comparison of matrix converters, and voltage-source converters for modern AC drives", *Industrial Electronics, IEEE Transactions on*, Vol.49, Issue 2, pp.304 – 314, April 2002.

[5] Kolar, J.W, Ertl, H, Zach, F.C, "Influence of the modulation method on the conduction and switching losses of a PWM converter system", *Industry Applications, IEEE Transactions on* Vol.27, Issue 6, pp. 1063 – 1075, Nov.-Dec. 1991.

[6] Schafmeister, F., Herold, S., Kolar, J.W., "Evaluation of 1200 V-Si-IGBTs and 1300 V-SiC-JFETs for application in three-phase very sparse matrix AC-AC converter systems", Applied Power Electronics Conference and Exposition, 2003. APEC '03. Eighteenth Annual IEEE, Vol. 1, pp. 241 – 255, 9-13 Feb. 2003.

[7] Schafmeister,F., Rytz, C., Kolar, J.W., "Analytical calculation of the conduction and switching losses of the conventional matrix converter and the (very) sparse matrix converter", Applied Power Electronics Conference and Exposition, 2005. APEC 2005. Twentieth Annual IEEE, Vol.2, pp. 875 – 881, 6-10 March 2005.

[8] F. Blaabjerg, U. Jaeger, S. Munk-Nielsen, and J. K. Pedersen, "Power losses in PWM–VSI inverter using NPT or PT IGBT devices", *IEEE Trans. Power Electron.*, Vol. 10, pp. 358–367, Mar. 1995.

[9] Robert W. Erickson, Dragan Maksimovic, *Fundamentals of Power Electronics*, Second Edition, Kluwer Academic Publishers, Massachusetts USA, Chap. 2, 2001.

[10] Fang Zheng Peng; "Z-source inverter", Industry Applications, *IEEE Transactions on*, Vol. 39, Issue 2, pp. 504 – 510, March-April 2003.

[11] Miaosen Shen, Jin Wang, Alan Joseph, Fang Z. Peng, Leon M. Tolbert, and Donald J. Adams, "Maximum Constant Boost Control of the Z-Source Inverter", Industry Applications Conference, 39th IAS Annual Meeting, IAS '2004, Conference Record of the 2004 IEEE , Vol. 1, pp.142 – 147, 2004.

[12] Alesina, A., Venturini, M.G.B., "Analysis and design of optimum-amplitude nine-switch direct AC-AC converters", *Power Electronics, IEEE Transactions on*, Vol. 4 , Issue 1 , pp.101 – 112, Jan. 1989.

[13] Holmes, D. G, Lipo, T. A., "Implementation of a controlled rectifier using AC-AC matrix converter theory", *Power Electronics, IEEE Transactions on*, Vol. 7, Issue 1, pp.240 – 250, Jan. 1992.

[14] Holmes, D.G.; "A unified modulation algorithm for voltage and current source inverters based on AC-AC matrix converter theory", *Industry Applications, IEEE Transactions on*, Vol. 28, Issue 1, pp. 31-40, Jan.-Feb. 1992.

[15] K. You and F. Rahman, "Analysis of conduction and switching losses of a matrix-Z-source converter", Power Electronics, 2007, ICPE'07 International Conference on, EXCO, Daegu, Korea, pp. 1071- 1076, 22-26, Oct. 2007.

Keping You (S'02-M'06) received his B.Sc. degree in Electrical Engineering from Harbin Institute of Technology, Harbin, China, in 1991. After working over one decade in China and Australia in the area of power electronics, he obtained his Ph.D. in Electrical Engineering from the University of New South Wales, Sydney, Australia, in 2008. He was an assistant engineer with the China Academy of Launch Vehicles from 1991 to 1995, an engineer in Mitsubishi Electric (Beijing Subsidiary) from 1995 to 1998, a senior technical engineer in International Rectifier Ltd (Beijing) from 1999 to 2001, and a testing engineer in Austest Laboratory, Sydney, Australia, in 2001. He is now working as a senior R&D engineer in Ampcontrol Pty Ltd, Australia. His research interests include applied power electronics and electric drives for automotive applications and renewable energy systems.

M. F. Rahman (M'78-SM'94) majored in Electrical Engineering in 1972 from the Bangladesh University of Engineering and Technology. He obtained his Masters and Ph.D. from the University of Manchester Institute of Science and Technology (UMIST), U. K., in 1975 and 1978, respectively. He subsequently worked as a systems design engineer at the General Electric Projects Co. of U. K. at Rugby, U/K., for two years before joining the National University of Singapore in 1980. He joined the University of New South Wales, Australia, in 1988 where he is now a full professor. His research interests are in electrical machines, power electronics, drives and associated control systems. He is a senior member of IEEE and is active in its Power Electronics, Industry Applications and Industrial Electronics societies.